Biochemical Engineering Journal 68 (2012) 85–90

Contents lists available at SciVerse ScienceDirect

Biochemical Engineering Journal

journal homepage: www.elsevier.com/locate/bej

Regular article

Analysis of mass transfer kinetics in the biosorption of synthetic dyes onto *Spirulina platensis* nanoparticles

G.L. Dotto, L.A.A. Pinto*

Unit Operation Laboratory, School of Chemistry and Food, Federal University of Rio Grande – FURG, 475 Engenheiro Alfredo Huch Street, 96203-900 Rio Grande, RS, Brazil

ARTICLE INFO

Article history:
Received 24 April 2012
Received in revised form 9 July 2012
Accepted 15 July 2012
Available online 21 July 2012

Keywords:
Biot number
Biosorption
Diffusion
Dyes
Mass transfer
Microalgae

ABSTRACT

In this research, the mass transfer kinetics for the biosorption of synthetic dyes (acid blue 9 and FD&C red no. 40) by *Spirulina platensis* nanoparticles was analyzed under different experimental conditions. The external mass transfer model (EMTM) and the homogeneous solid diffusion model (HSDM) were employed to study the mass transfer kinetics and also to estimate the values of external mass transfer coefficient (k_f) and intraparticle diffusion coefficient (D_{int}). The Biot number (Bi) was used to verify the importance of external mass transfer in relation to intraparticle diffusion. The values of external mass transfer coefficient (k_f) ranged from 1.67×10^{-6} to 11.40×10^{-6} cm s^{-1} and the intraparticle diffusion coefficient (D_{int}) ranged from 0.70×10^{-14} to 4.30×10^{-14} cm^2 s^{-1}. The Biot numbers ($0.53 \leq Bi \leq 10.33$) showed that, for both dyes, the biosorption onto *S. platensis* nanoparticles was controlled simultaneously by external mass transfer and intraparticle diffusion.

1. Introduction

The inadequate disposal of wastewaters originated from dye production and application present a very serious environmental problem [1], being a risk to the aquatic ecosystems and to human health [2,3]. Many methods have been employed to remove synthetic dyes from industrial effluents [3–5]. Among these methods, the biosorption is an emergent, competitive, effective and inexpensive technology which reduces the concentration of synthetic dyes to acceptable levels [5–9]. For this purpose, various biosorbents, such as, fungi, bacteria, chitosan, peat and algae are reported in the literature [2,5–11]. Recently, the microalgae *Spirulina platensis* was proposed as an alternative biosorbent to removal dyes from wastewater [9,12,13], however, researches about its application are limited.

S. platensis is available in large quantities, is largely cultivated throughout worldwide and relatively cheap [14–16]. In addition, its biomass contains a variety of functional groups, such as, carboxyl, hydroxyl, sulfate and other charged groups which can be responsible for pollutants binding [9,12,16–18]. These characteristics show that the *S. platensis* is a promising biosorbent [16–18]. However, all properties of *S. platensis* are not accessible in the natural form of the biomass. In this way, our research group has prepared *S. platensis* nanoparticles to improve its biosorption proprieties [12]. In our recent study [12], the equilibrium and thermodynamics for the biosorption of food dyes onto *S. platensis* nanoparticles were elucidated, but there is no information in the literature about the mass transfer kinetics of dyes biosorption onto *S. platensis* nanoparticles.

In biosorption systems, it is fundamental the study of the mass transfer kinetics and the potential rate controlling steps [5]. From this analysis, the solute uptake rate, which determines the residence time required for completion of biosorption reaction, may be established [5,19]. Biosorption mass transfer kinetics must consider the three following steps: external mass transfer, intraparticle diffusion and uptake of molecules by the active sites [5,20–22]. Generally, for dye removal by biosorbents, this last step is very fast [5,7,9,12], so, the process is controlled by external mass transfer or/and intraparticle diffusion. These steps can be affected by various factors [5,7,11,20,22], being important verify its influences for design purposes.

This work aimed to elucidate the mass transfer kinetics of the synthetic dyes (acid blue 9 and FD&C red no. 40) biosorption onto *S. platensis* nanoparticles. The nanoparticles were obtained from *S. platensis* dead biomass and characterized by dynamic light scattering (DLS), N_2-adsorption isotherms (BET method) and scanning electron microscopy (SEM). The mass transfer kinetics was analyzed under different conditions of pH (2–4) and stirring rate (50–400) by the external mass transfer (EMTM) and the homogeneous solid diffusion (HSDM) models.

* Corresponding author. Tel.: +55 53 3233 8645; fax: +55 53 3233 8745.
E-mail addresses: guilherme_dotto@yahoo.com.br (G.L. Dotto), dqmpinto@furg.br (L.A.A. Pinto).

1369-703X/$ – see front matter © 2012 Elsevier B.V. All rights reserved.
http://dx.doi.org/10.1016/j.bej.2012.07.010

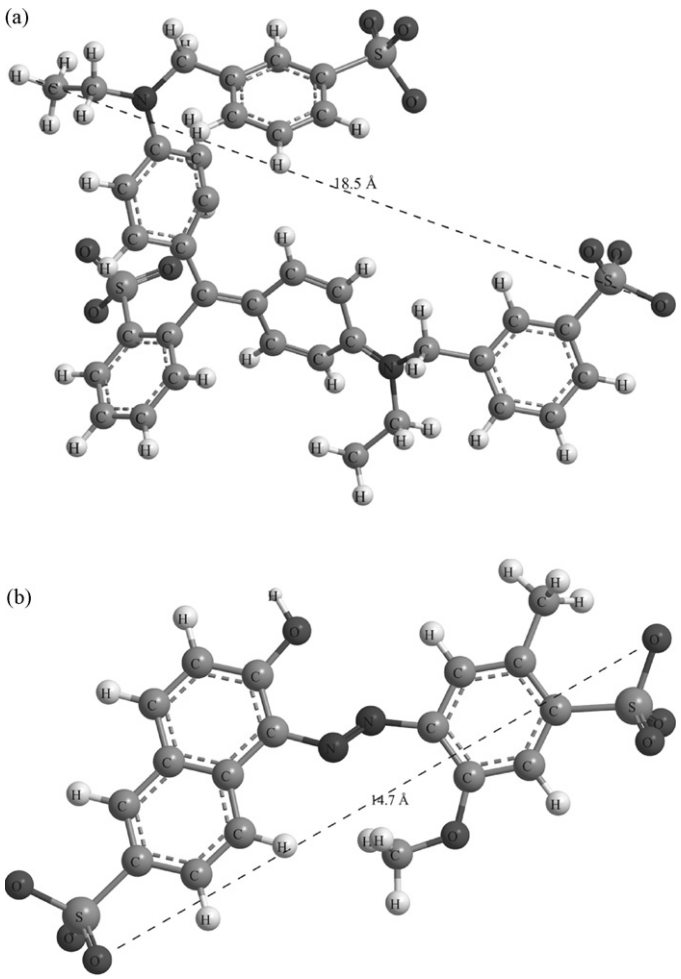

Fig. 1. Optimized three-dimensional structural formulae of the dyes: (a) acid blue 9 and (b) FD&C red no. 40.

2. Materials and methods

2.1. Dyes

The synthetic dyes acid blue 9 (triphenylmethane dye, molecular weight 792.8 g mol^{-1}, color index 42,090, λ_{max} = 408 nm, pK_a = 5.6 and 6.6) and FD&C red no. 40 (azo dye, molecular weight 496.4 g mol^{-1}, color index 16,045, λ_{max} = 500 nm, pK_a = 11.4) were supplied by local manufacturer, Plury Chemical Ltd., with a purity higher than 85%. The optimized three-dimensional structural formulae of the dyes (obtained from ChemBio 3D 11.0.1 software (Cambridge Soft, USA)) are shown in Fig. 1. The dyes wavelength is constant with the pH. Distilled water was used to prepare all solutions. All reagents were of analytical-grade.

2.2. Preparation and characterization of S. platensis nanoparticles

S. platensis nanoparticles were prepared by a previously reported mechanical agitation method [12]. In summary, *S. platensis* strain LEB-52 was cultivated in a 450 L open outdoor photobioreactors, being the biomass recovered with a moisture content of 0.76 kg kg^{-1} (wet basis) [23]. The wet biomass was dried [24], ground (Wiley Mill Standard, no. 03, USA) and sieved until the discrete particle size ranged from 68 to 75 μm. The sieved biomass (250 mg) was added in distilled water (90 mL) and the pH was adjusted (2, 3 and 4) using 10 mL of a buffer disodium phosphate/citric acid solution (0.1 mol L^{-1}). The suspension was agitated (Dremel, 1100-01, Brazil) at 10,000 rpm for 20 min [12]. Detailed information can be obtained in the literature [12,23,24].

The mean diameter (d_p) and polydispersity index (PDI) of the nanoparticles were obtained by dynamic light scattering (DLS) [25]. The dynamic light scattering equipment was constituted by a laser (Spectra-physics, 127, USA) coupled to a goniometer (Brookheaven, BI-200M, USA) and a digital correlator (Brookheaven, BI-9000AT, USA).

The specific surface area, pore volume and average pore radius of the nanoparticles were obtained by a volumetric adsorption analyzer (Quantachrome Instruments, New Win 2, USA) using the Bennett, Emmet and Teller (BET) method [26]. The apparent density and void fraction of the nanoparticles were estimated by the following equations [26]:

$$V_p = \frac{1}{\rho_p} - \frac{1}{\rho_s} \quad (1)$$

$$\varepsilon_p = 1 - \frac{\rho_p}{\rho_s} \quad (2)$$

where ρ_p is the apparent density (kg m^{-3}), ρ_s is the solid density (kg m^{-3}), V_p is the pore volume (m^3 kg^{-1}) and ε_p is the void fraction.

In order to verify the surface morphology of *S. platensis* nanoparticles, and also to confirm its mean diameter, images were obtained from scanning electron microscopy (SEM) (Jeol, JSM-6060, Japan) [8].

2.3. Biosorption experiments

The biosorption experiments were carried out using batch systems at different values of pH (2, 3 and 4) and stirring rate (50, 225 and 400 rpm) (These values were determined from the literature and preliminary tests.). Firstly, 100 mL of a suspension containing 250 mg of *S. platensis* nanoparticles had the pH adjusted (2, 3 and 4) (Mars, MB10, Brazil) through the 50 mL of buffer disodium phosphate/citric acid solution (0.1 mol L^{-1}), which did not present interaction with the dyes [10]. After, 50 mL of a solution containing 10 g L^{-1} of dye was added to each *S. platensis* suspension, and it was completed to 1 L with distilled water, thus, the initial dye concentration was approximately 500 mg L^{-1}.

The experiments were carried out in a jar test (Nova etica, 218 MBD, Brazil), under ambient temperature (25 ± 1 °C) [12]. Aliquots were withdrawn in preset time intervals (2, 4, 6, 8, 10, 15, 20, 25, 30, 40, 60, 80, 100 and 120 min). The biomass and biosorbed dyes were removed from the liquid through a filtration with Whatmann Filter Paper no. 40, which did not present interaction with the dyes [10], and the dyes concentration was determined by spectrophotometry (Quimis, Q108, Brazil). All experiments were carried out in replicate (n = 3) and blanks were performed.

The mean biosorption capacity at time "t" (q_t) (mg g^{-1}) was calculated as follows:

$$q_t = \frac{C_0 - C_t}{m} V \quad (3)$$

where C_0 is the initial dye concentration in liquid phase (mg L^{-1}), C_t is the dye concentration in liquid phase at time t (mg L^{-1}), m is biosorbent amount (g) and V is the volume of suspension (L).

2.4. Analysis of mass transfer kinetics

In this work, the mass transfer kinetics was analyzed as follows: Firstly, to identify the different mass transfer steps that occur in the biosorption process, the experimental values of "q_t" were plotted as a function of "$t^{0.5}$" [27]. After, EMTM (external mass transfer model) and HSDM (homogeneous solid diffusion model) models were fitted with the experimental data (first and second linear portions,

respectively) in order to estimate the external mass transfer coefficient (k_f) and the intraparticle diffusion coefficient (D_{int}). Finally, the Biot number (Bi) was calculated to verify the relative importance of external mass transfer to intraparticle diffusion [28,29].

The EMTM is based upon the assumption that the external mass transport is controlling the overall rate of biosorption [26]. According to Suzuki [28], in this case, the solute concentration in the particle is assumed to be uniform, and the mass transfer can be represented by the following equation:

$$\frac{dC_t}{dt} = -k_f S_A (C_t - C_s) \quad (4)$$

where C_s is the solute concentration at the external surface of the biosorbent (mg L^{-1}), k_f is the external mass transfer coefficient (cm s^{-1}) and S_A (cm^{-1}) is defined as follows:

$$S_A = \frac{6(m/V)}{d_p \rho_p (1 - \varepsilon_p)} \quad (5)$$

When $t \to 0$, $C_s \to 0$ and $C_t \to C_0$, this manner, Eq. (4) can be integrated leading to [28]:

$$\frac{C_t}{C_0} = \exp(-k_f S_A t) \quad (6)$$

In this way, Eq. (6) can be fitted to the experimental data to check the biosorption mechanism, and also the k_f values can be estimated.

When mass transfer resistance is internal, intraparticle diffusion controls the process. In this case, the HSDM can describe the mass transfer in an amorphous and homogeneous sphere [28] for a unidirectional and isothermal process [29]. If intraparticle diffusivity is considered constant, the HSDM can be presented in the form of [28]:

$$\frac{\partial q}{\partial t} = \left(\frac{D_{int}}{r^2}\right) \frac{\partial}{\partial r}\left(r^2 \frac{\partial q}{\partial r}\right) \quad (7)$$

where D_{int} is the intraparticle diffusion coefficient (cm^2 s^{-1}), r is the radial position (cm), and q the biosorption quantity of solute in the solid (mg g^{-1}) varying with radial position at time t. The initial and boundary conditions are presented as follows [22,28,29]:

$$q(r, 0) = 0 \quad (8)$$

$$q\left(\frac{d_p}{2}, t\right) = q_e \quad (9)$$

$$\left(\frac{\partial q}{\partial r}\right)_{r=0} = 0 \quad (10)$$

where q_e is the biosorption capacity at equilibrium (mg g^{-1}).

The balance for the batch system is given by Eq. (11) [28]:

$$V\left(\frac{dC}{dt}\right) = -m\left(\frac{dq_t}{dt}\right) \quad (11)$$

In the concentration range of this work, the Henry model showed a good fit with the equilibrium experimental data in the biosorption of both dyes onto *S. platensis* nanoparticles (see Supplementary material). Then, the relationship between the equilibrium concentrations of the fluid phase and biosorbed phase can be considered linear. In this case, for finite volume process, Crank [30] developed a solution for Eq. (7), which can be approximated to the first term of series when the Fourier number is higher than 0.2:

$$\frac{q_t}{q_e} = 1 - \left[\frac{6\alpha(\alpha+1)\exp(-q_n^2 D_{int} t/R_p^2)}{9 + 9\alpha + q_n^2\alpha^2}\right] \quad (12)$$

where R_p is the particle radius (cm), α is the effective volume ratio, expressed as a function of the equilibrium partition coefficient (solid/liquid concentration ratio) ($C_e/C_0 - C_e$) and q_n can be obtained as follows:

$$\tan\ q_n = \frac{3q_n}{3 + \alpha q_n^2} \quad (13)$$

This manner, from Eq. (8) it is possible to estimate the intraparticle diffusion coefficient (D_{int}) values.

The influence of each mass transfer step on the dye biosorption resistance was found by a non-dimensional Biot number (Bi), which reflects the relative importance of external mass transfer to intraparticle diffusion. The Biot number is defined as follows [31]:

$$\mathrm{Bi} = \frac{k_f d_p C_0}{2\rho_p D_{int} q_0} \quad (14)$$

where q_0 (mg g^{-1}) is the solid phase concentration in the biosorbent in equilibrium with a residual hypothetical liquid concentration.

Table 1
Characteristics of *S. platensis* nanoparticles.

Characteristic	Value[a]
Polydispersity index (PDI)	0.150 ± 0.010
Mean diameter (d_p) (nm)	215 ± 10
Specific surface area (S_S) (m^2 g^{-1})	14.0 ± 0.1
Pore volume (V_p) (m^3 kg^{-1}) × 10^6	6.9 ± 0.1
Average pore radius (A_R) (Å)	23.0 ± 0.2
Solid density (ρ_s) (kg m^{-3})	1391.5 ± 1.2
Apparent density (ρ_p) (kg m^{-3})	1378.3 ± 1.5
Void fraction (ε_p)	0.010 ± 0.002

[a] Mean ± standard error in triplicate.

2.5. Non-linear regression analysis

The mass transfer coefficients (k_f and D_{int}) were determined from the fit of the models to the experimental data by non-linear regression, using Statistic 7.0 software (Statsoft, USA) through Quasi-Newton estimation method. The fit quality was measured by the coefficient of determination (R^2) and average relative error (ARE).

3. Results and discussion

3.1. Characteristics of S. platensis nanoparticles

The characteristics of *S. platensis* nanoparticles are shown in Table 1. The PDI value (Table 1) shows that the *S. platensis* nanoparticles were stable, relatively monodisperse and presented a little variation in the size. According to Bruce and Pecora [32], a near-monodisperse system would have a PDI value of 0.2 or lower. Fig. 2 shows the SEM images of *S. platensis* nanoparticles. In Fig. 2 is shown that *S. platensis* nanoparticles presented a size distribution in the range from 50 to 500 nm. Nanoparticles are commonly described as solid colloidal particles, ranging in size from 10 nm to 1000 nm [32]. In addition, it can be observed in Fig. 2 that the nanoparticles were homogeneous, with ellipsoidal–spherical forms.

3.2. Mass transfer kinetics

To identify the mass transfer steps that occur in the biosorption process, the biosorption capacity as a function of the square root of time was plotted [27,33]. According to Weber and Morris [27], the plot q_t versus $t^{0.5}$ shows multi-linearity, and each portion represents a distinct mass transfer step. The first portion is the external mass transfer or instantaneous adsorption step. The second portion is the gradual adsorption step where the intraparticle diffusion can be rate controlling. The third portion is the final equilibrium [27]. The Weber–Morris plots of the acid blue 9 and FD&C red no. 40

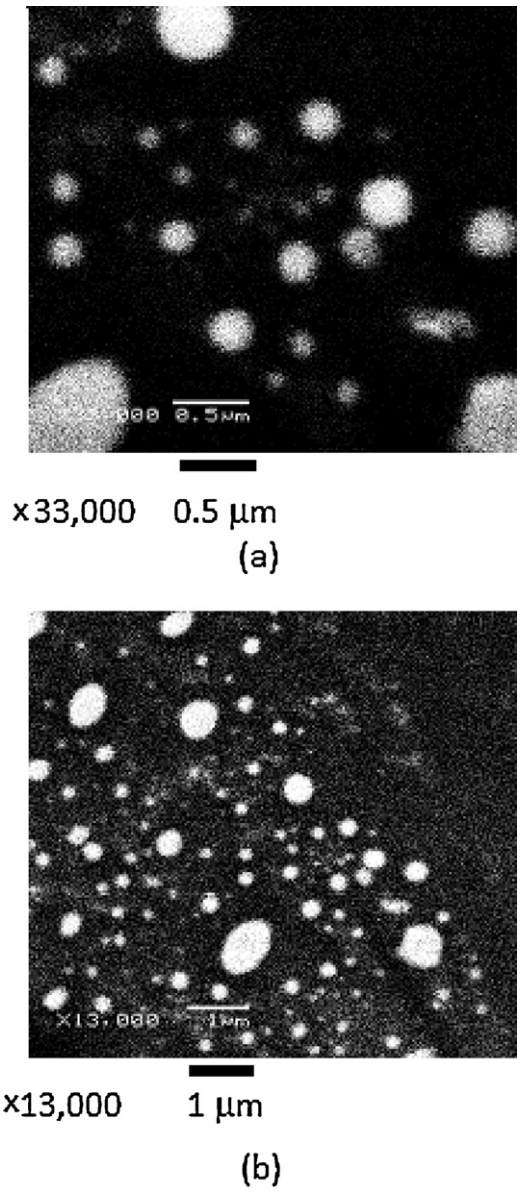

Fig. 2. SEM images of *S. platensis* nanoparticles: (a) 33,000×; (b) 13,000×.

biosorption onto *S. platensis* nanoparticles under different conditions of pH and stirring rate are shown in Figs. 3 and 4, respectively (the curves of C_t versus time at the same conditions are presented in Supplementary material).

Figs. 3 and 4 presented the multi-linearity with two distinct phases. The initial portion is relative to the external mass transfer. The second portion describes the gradual biosorption step, where intraparticle diffusion control is rate limiting. This shows that the external mass transfer and intraparticle diffusion occurred simultaneously during the biosorption of acid blue 9 and FD&C red no. 40 onto *S. platensis* nanoparticles.

In order to estimate the external mass transfer coefficient (k_f) and the intraparticle diffusion coefficient (D_{int}), the experimental data of the first portion of Weber–Morris plot were fitted with the EMTM (Eq. (6)), and experimental data of second portion were fitted with HSDM (Eq. (12)). The mass transfer coefficients (k_f and D_{int}) and Biot number (Eq. (14)) for the synthetic dyes biosorption onto *S. platensis* nanoparticles are shown in Table 2.

As can be seen in Table 2, the external mass transfer model (EMTM) presented good fit with the experimental data in

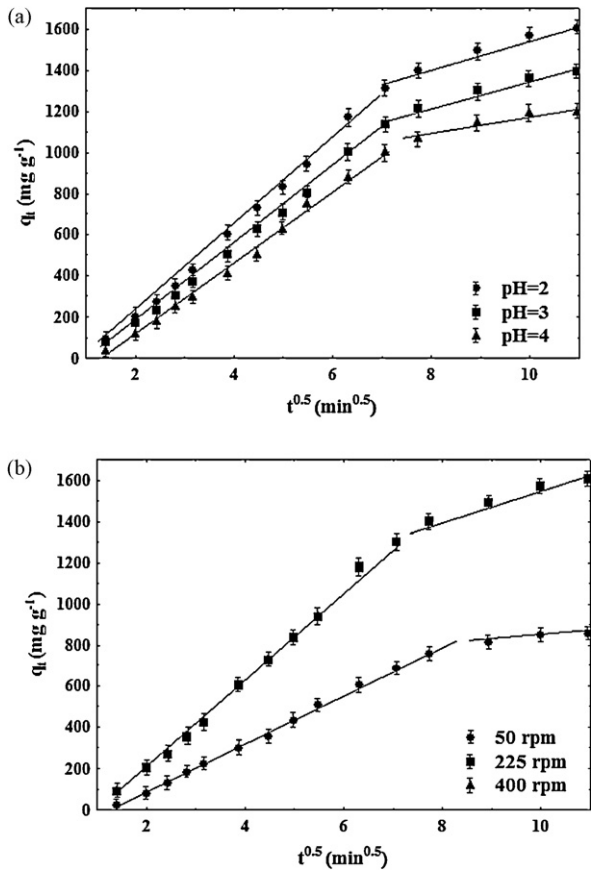

Fig. 3. Weber–Morris plots of acid blue 9 biosorption onto *S. platensis* nanoparticles: (a) pH effect (400 rpm) and (b) stirring rate effect (pH 2).

relation to the first portion of the Weber–Morris plot ($R^2 > 0.95$ and ARE < 4.00%). In the same way, the HSDM model presented good fit with the experimental data for the second portion of the Weber–Morris plot ($R^2 > 0.95$ and ARE < 8.00%). In Table 2, three aspects can be noted in relation to the k_f values. First aspect, in general, the k_f values were increased with the pH decrease. This suggests that the pH decrease lead to an increase in biosorption rate, and consequently, the contribution of external mass transfer is decreased. This occurred because in low values of pH, the dyes sulfonated groups were more rapidly dissociated; in addition, the *S. platensis* surface is easily protonated, consequently, the electrostatic attraction was increased, facilitating the mass transfer in the external layer. The same dependence of k_f with the pH was demonstrated by Piccin et al. [34]. Second aspect, the stirring rate increase caused an increase in the k_f values. This occurred because the stirring rate increase causes an increase in the energy dissipation and turbulence in the mixing zone, leading to an increase in system mobility. This manner, a decrease in the external film thickness occurs, decreasing the external resistance and consequently, facilitating the transference across the external layer. Similar behavior was obtained by other researches [11,20,26]. Third aspect, the k_f values for the acid blue 9 were lower than k_f values for the FD&C red no. 40. This can be occurred because acid blue 9 had a higher and more ramified molecular structure (Fig. 1). As consequence, its molecular diffusivity is lower [28,29], hindering the transference across the external layer.

The intraparticle diffusion coefficient values not presented tendency in relation to the pH and stirring rate, however, in general were higher for the FD&C red no. 40 (Table 2). This can be occurred because FD&C red no. 40 had a lower molecular structure (Fig. 1), facilitating its transference inside of the *S. platensis* nanoparticles.

Table 2
Mass transfer coefficients (k_f and D_{int}) and Biot number (Bi) for the synthetic dyes biosorption onto *S. platensis* nanoparticles.

Dye	pH	Stirring rate (rpm)	EMTM			HSDM			Biot number
			k_f ($\times 10^6$ cm s^{-1})	R^2	ARE (%)	D_{int} ($\times 10^{14}$ cm^2 s^{-1})	R^2	ARE (%)	
Acid blue 9	2	50	2.68	0.972	2.01	0.70	0.955	6.78	0.95
		225	6.68	0.994	1.28	2.10	0.993	0.21	0.80
		400	6.75	0.994	1.35	2.09	0.998	0.12	0.81
	3	50	2.74	0.968	2.14	0.75	0.954	7.54	1.05
		225	3.59	0.977	2.44	0.97	0.954	4.56	1.07
		400	5.38	0.988	1.50	1.94	0.999	0.78	0.80
	4	50	1.67	0.956	1.88	1.03	0.999	0.17	0.53
		225	2.86	0.968	2.23	1.55	0.961	5.23	0.60
		400	4.41	0.993	1.29	1.17	0.962	2.82	1.22
FD&C red no. 40	2	50	8.19	0.994	0.24	3.21	0.992	1.15	2.46
		225	9.97	0.955	0.90	2.36	0.992	2.73	4.07
		400	11.40	0.986	0.52	1.92	0.996	1.45	5.73
	3	50	3.59	0.958	0.31	4.30	0.979	6.26	1.04
		225	9.51	0.957	3.50	1.15	0.967	7.35	10.33
		400	10.80	0.965	0.82	1.37	0.971	3.23	9.89
	4	50	1.75	0.958	0.45	1.82	0.988	5.39	1.65
		225	7.81	0.957	2.30	1.65	0.998	1.01	8.14
		400	9.32	0.994	0.18	1.66	0.979	5.44	9.65

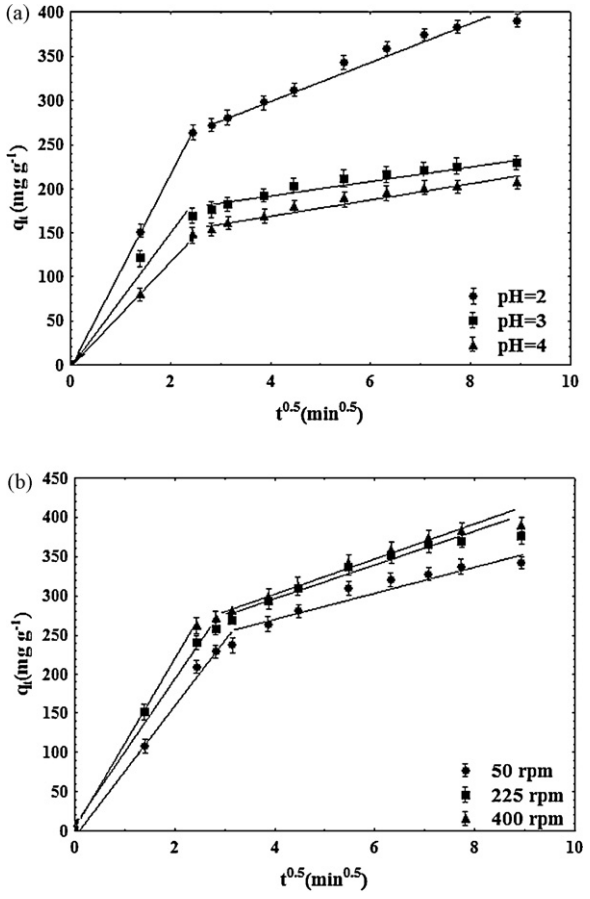

Fig. 4. Weber–Morris plots of FD&C red no. 40 biosorption onto *S. platensis* nanoparticles: (a) pH effect (400 rpm) and (b) stirring rate effect (pH 2).

Similar behavior was obtained by Leyva-Ramos et al. [26] in the adsorption of organic compounds on activated carbon cloth. The intraparticle diffusion coefficient values obtained in this research were in the range of 10^{-14} cm^2 s^{-1} (Table 2). Intraparticle diffusion coefficient values in the range from 10^{-14} to 10^{-11} cm^2 s^{-1} were obtained by Sushanta and Uday [35] in the adsorption of Cr(III) and Cr(VI) from aqueous solutions by crystalline titanium oxide.

In Table 2, it was observed that the Biot numbers for the acid blue 9 were lower than the Biot numbers for the FD&C red no. 40. This shows that the external mass transfer was more important in the biosorption of acid blue 9. In spite of this, for the biosorption of both dyes, the external mass transfer and intraparticle diffusion should be considered. For Bi < 0.5, it exists a complete dominance of the external resistance, while for Bi > 10, the external mass transfer can be neglected, and considerable dominance of the intraparticle resistance exists [31,36]. On the basis in the Biot numbers presented in Table 2, it can be affirmed that the biosorption was controlled simultaneously by external mass transfer and intraparticle diffusion.

4. Conclusion

The mass transfer kinetics for the biosorption of synthetic dyes (acid blue 9 and FD&C red no. 40) by *S. platensis* nanoparticles was analyzed at different conditions of pH and stirring rate. For both dyes, the biosorption occurred by external mass transfer and intraparticle diffusion. The pH decrease and the stirring rate increase caused an increase in the k_f values, which varied from 1.67×10^{-6} to 11.40×10^{-6} cm s^{-1}. The intraparticle diffusivity values not presented tendency in relation to the pH and stirring rate, with range from 0.70×10^{-14} to 4.30×10^{-14} cm^2 s^{-1}. The Biot numbers ($0.53 \leq Bi \leq 10.33$) showed that the biosorption was controlled simultaneously by external mass transfer and intraparticle diffusion.

Acknowledgments

The authors would like to thank CAPES (Brazilian Agency for Improvement of Graduate Personnel) and CNPq (National Council of Science and Technological Development) for the financial support.

Appendix A. Supplementary data

Supplementary data associated with this article can be found, in the online version, at http://dx.doi.org/10.1016/j.bej.2012.07.010.

References

[1] N. Koprivanac, H. Kusic, Hazardous Organic Pollutants in Colored Wastewaters, New Science Publishers, New York, 2008.

[2] A. Srinivasan, T. Viraraghavan, Decolorization of dye wastewaters by biosorbents: a review, J. Environ. Manag. 91 (2010) 1915–1929.
[3] V.K. Gupta, Suhas, Application of low-cost adsorbents for dye removal: a review, J. Environ. Manag. 90 (2009) 2313–2342.
[4] S. Mondal, Methods of dye removal from dye house effluent: an overview, Environ. Eng. Sci. 25 (2008) 383–396.
[5] Z. Aksu, Application of biosorption for the removal of organic pollutants: a review, Proc. Biochem. 40 (2005) 997–1026.
[6] I. Kiran, T. Akar, A.S. Ozcan, A. Ozcan, S. Tunali, Biosorption kinetics and isotherm studies of Acid Red 57 by dried *Cephalosporium aphidicola* cells from aqueous solutions, Biochem. Eng. J. 31 (2006) 197–203.
[7] S.V. Mohan, S.V. Ramanaiah, P.N. Sarma, Biosorption of direct azo dye from aqueous phase onto *Spirogyra* sp. *I02*: evaluation of kinetics and mechanistic aspects, Biochem. Eng. J. 38 (2008) 61–69.
[8] W. Cheng, S.G. Wang, L. Lu, W.X. Gong, X.W. Liu, B.Y. Gao, H.Y. Zhang, Removal of malachite green (MG) from aqueous solutions by native and heat-treated anaerobic granular sludge, Biochem. Eng. J. 39 (2008) 538–546.
[9] G.L. Dotto, V.M. Esquerdo, M.L.G. Vieira, L.A.A. Pinto, Optimization and kinetic analysis of food dyes biosorption by *Spirulina platensis*, Colloids Surf. B: Biointerfaces 91 (2012) 234–241.
[10] G.L. Dotto, L.A.A. Pinto, Adsorption of food dyes onto chitosan: optimization process and kinetic, Carbohydr. Polym. 84 (2011) 231–238.
[11] G.L. Dotto, L.A.A. Pinto, Adsorption of food dyes acid blue 9 and food yellow 3 onto chitosan: stirring rate effect in kinetics and mechanism, J. Hazard. Mater. 187 (2011) 164–170.
[12] G.L. Dotto, E.C. Lima, L.A.A. Pinto, Biosorption of food dyes onto *Spirulina platensis* nanoparticles: equilibrium isotherm and thermodynamic analysis, Bioresour. Technol. 103 (2012) 123–130.
[13] A. Çelekli, M. Yavuzatmaca, E. Beyazçiçek, H. Bozkurt, Effect of initial reactive red 120 concentrations on the biomass production and dye uptake by *Spirulina platensis*, Fresen. Environ. Bull. 16 (2009) 994–998.
[14] G. Markou, D. Georgakakis, Cultivation of filamentous cyanobacteria (blue-green algae) in agro-industrial wastes and wastewaters: a review, Appl. Energy 88 (2011) 3389–3401.
[15] J.A.V. Costa, M.G. Morais, The role of biochemical engineering in the production of biofuels from microalgae, Bioresour. Technol. 102 (2011) 2–9.
[16] A. Çelekli, M. Yavuzatmaca, H. Bozkurt, An eco-friendly process: predictive modeling of copper adsorption from aqueous solution on *Spirulina platensis*, J. Hazard. Mater. 173 (2010) 123–129.
[17] A. Seker, T. Shahwan, A. Erŏglu, S. Yilmaz, Z. Demirel, M. Dalay, Equilibrium, thermodynamic and kinetic studies for the biosorption of aqueous lead(II), cadmium(II) and nickel(II) ions on *Spirulina platensis*, J. Hazard. Mater. 154 (2008) 973–980.
[18] S.V. Gokhale, K.K. Jyoti, S.S. Lele, Modeling of chromium (VI) biosorption by immobilized *Spirulina platensis* in packed column, J. Hazard. Mater. 170 (2009) 735–743.
[19] H. Qiu, L.L. Pan, Q.J. Zhang, W. Zhang, Q. Zhang, Critical review in adsorption kinetic models, J. Zhejiang Univ. Sci. A 10 (2009) 716–724.
[20] R. Ocampo-Perez, R. Leyva-Ramos, J. Mendoza-Barron, R.M. Guerrero-Coronado, Adsorption rate of phenol from aqueous solution onto organobentonite: surface diffusion and kinetic models, J. Colloid Interface Sci. 364 (2011) 195–204.
[21] R.B. Garcia-Reyes, J.R. Rangel-Mendez, Adsorption kinetics of chromium (III) ions on agro-waste materials, Bioresour. Technol. 101 (2010) 8099–8108.
[22] C. Costa, A.E. Rodrigues, Intraparticle diffusion of phenol in macroreticular adsorbents: modelling and experimental study of batch and CSTR adsorbers, Chem. Eng. Sci. 40 (1985) 983–993.
[23] J.A.V. Costa, L.M. Colla, P.F.F. Duarte, Improving *Spirulina platensis* biomass yield using a fed-batch process, Bioresour. Technol. 92 (2004) 237–241.
[24] E.G. Oliveira, G.S. Rosa, M.A. Moraes, L.A.A. Pinto, Characterization of thin layer drying of *Spirulina platensis* utilizing perpendicular air flow, Bioresour. Technol. 100 (2009) 1297–1303.
[25] S.K. Brar, M. Verma, Measurement of nanoparticles by light-scattering techniques, Trends Anal. Chem. 30 (2011) 4–17.
[26] R. Leyva-Ramos, R. Ocampo-Perez, J. Mendoza-Barron, External mass transfer and hindered diffusion of organic compounds in the adsorption on activated carbon cloth, Chem. Eng. J. 183 (2012) 141–151.
[27] W.J. Weber, J.C. Morris, Kinetics of adsorption of carbon from solutions, J. Sanit. Eng. Div. Am. Soc. Civ. Eng. 89 (1963) 31–63.
[28] M. Suzuki, Adsorption Engineering, Kodansha, Tokyo, 1990.
[29] D.M. Ruthven, Principles of Adsorption and Adsorption Processes, John Wiley & Sons, New York, 1984.
[30] J. Crank, The Mathematics of Diffusion, Clarendon Press, Oxford, 1975.
[31] D.O. Cooney, Comparison of simple adsorber breakthrough curve method with exact solution, Am. Inst. Chem. Eng. J. 39 (1993) 355–358.
[32] J. Bruce, R. Pecora, Dynamic Light Scattering: With Applications to Chemistry, Biology and Physics, Dover publications, New York, 2000.
[33] M.I. El-Khaiary, G.F. Malash, Common data analysis errors in batch adsorption studies, Hydrometallurgy 105 (2011) 314–320.
[34] J.S. Piccin, G.L. Dotto, M.L.G. Vieira, L.A.A. Pinto, Kinetics and mechanism of the food dye FD&C red no. 40 adsorption onto chitosan, J. Chem. Eng. Data 56 (2011) 3759–3765.
[35] D. Sushanta, C.G. Uday, Kinetics, isotherm and thermodynamics for Cr(III) and Cr(VI) adsorption from aqueous solutions by crystalline hydrous titanium oxide, J. Chem. Thermodyn. 40 (2008) 67–77.
[36] P. Li, G. Xiu, A.E. Rodrigues, Modeling separation of proteins by inert core adsorbent in a batch adsorber, Chem. Eng. Sci. 58 (2003) 3361–3371.